Preliminary Results from Long-Term Measurements of Atmospheric Moisture in the Marine Boundary Layer in the Gulf of Mexico*

LAURENCE C. BREAKER

National Weather Service, NCEP, NOAA, Washington, D.C.

DAVID B. GILHOUSEN

National Weather Service, National Data Buoy Center, NOAA, Stennis Space Center, Mississippi

LAWRENCE D. BURROUGHS

National Weather Service, NCEP, NOAA, Washington, D.C.

(Manuscript received 1 April 1997, in final form 18 July 1997)

ABSTRACT

Measurements of boundary layer moisture have been acquired from Rotronic MP-100 sensors deployed on two National Data Buoy Center (NDBC) buoys in the northern Gulf of Mexico from June through November 1993. For one sensor that was retrieved approximately 8 months after deployment and a second sensor that was retrieved about 14 months after deployment, the pre- and postcalibrations agreed closely and fell within WMO specifications for accuracy. A second Rotronic sensor on one of the buoys provided the basis for a detailed comparison of the instruments and showed close agreement. A separate comparison of the Rotronic instrument with an HO-83 hygrometer at NDBC showed generally close agreement over a 1-month period, which included a number of fog events. The buoy observations of relative humidity and supporting data from the buoys were used to calculate specific humidity. Specific humidities from the buoys were compared with specific humidities computed from observations obtained from nearby ship reports, and the correlations were generally high (0.7–0.9). Uncertainties in the calculated values of specific humidity were also estimated and ranged between 0.27% and 2.1% of the mean value, depending on the method used to estimate this quantity.

The time series of specific humidity revealed three primary scales of variability: small scale (of the order of hours), synoptic scale (several days), and seasonal (several months). The synoptic-scale variability was clearly dominant; it was eventlike in character and occurred primarily during September, October, and November. Most of the synoptic-scale variability was due to frontal systems that dropped down into the Gulf of Mexico from the continental United States, followed by air masses that were cold and dry. One particularly intense event on 30 October 1993 was chosen for a more detailed analysis in terms of the characteristic return-flow cycles that occur in the northern Gulf of Mexico during fall and winter. Finally, cross-correlation analyses of the buoy data indicated that the prevailing weather systems generally entered the buoy domain from the south prior to September; thereafter, they became more coherent and tended to enter the region from the north.

1. Introduction

The acquisition of meteorological observations within the marine boundary layer has always posed unique problems due to the proximity of the ocean surface to the sensor location and the constant state of motion of the surface itself. Atmospheric humidity has been a particularly difficult parameter to measure near the ocean surface. First, it is difficult to protect humidity sensors from salt spray that accumulates over time and consequently degrades calibration accuracy; second, humidity sensors must be adequately protected from excess heating due to incoming solar radiation; and finally, humidity sensors must recover from periods of saturation rapidly and without change to their calibration (Coantic and Friehe 1980).

Since atmospheric moisture is a difficult parameter to measure accurately over the ocean, it is not surprising that it has been even more difficult to acquire observations of boundary layer moisture from unattended instruments for extended periods of several months or more. Recently, however, a number of humidity sensors were evaluated for possible use in measuring atmospheric moisture in the marine environment (e.g., Sem-

---

mer 1987; Muller and Beekman 1987; Crescenti et al. 1990; Katsaros et al. 1994).

Because of the continuing need for long-term measurements of moisture within the marine boundary layer, the National Data Buoy Center (NDBC) evaluated the Rotronic MP-100 humidity sensor for possible deployment on their moored ocean data buoys, based on promising test results from Muller and Beekman (1987) and Semmer (1987). Initial field tests were conducted along the U.S. west coast in 1989. A Rotronic humidity sensor was installed on a Coastal-Marine Automated Network (C-MAN) station at Point Arguello, California. Calculated dewpoint temperatures following fog events were in general agreement with those reported at nearby Vandenberg Air Force Base and showed high correlations between saturation events and restricted visibilities in fog. After a 4-month evaluation, Rotronic humidity sensors were introduced on several NDBC buoys and C-MAN stations along the California coast. Initially, several gross failures occurred within weeks after installation. A gross failure occurred when reported relative humidities either 1) exceeded 106%,[1] 2) remained at, or exceeded, 100% for a day or more after satellite imagery indicated fog dissipation, or 3) disagreed by 30% or more with nearby reports for values of relative humidity, which were typically less than 30%.

These failures led to several improvements to the Rotronic sensor and its installation aboard the NDBC buoy platforms. First, the cabling from the sensor to the on-board electronic payload was replaced. The original cables had inadequate insulation, and cable flexing often produced large calibration shifts. Second, the method of calibration was improved twice. The first improvement consisted of exposing the sensor to a series of different saturated salt solutions in closed flasks and then comparing the observed relative humidities to the known equilibrium vapor pressure of water at the observed temperatures for these solutions. Test flasks with relative humidities ranging from 11% to 96% were used. Then, when this method proved tedious, NDBC purchased a chamber with better humidity regulation and one that is now traceable to the National Institute of Standards and Technology. These improvements led to significantly greater measurement accuracy and sensor reliability. As a result, these instruments have been installed on a number of NDBC buoys since 1989, concomitant with improvements in their performance.

As a basis for this study, hourly measurements of relative humidity and other supporting environmental data were acquired from two NDBC buoys in the Gulf
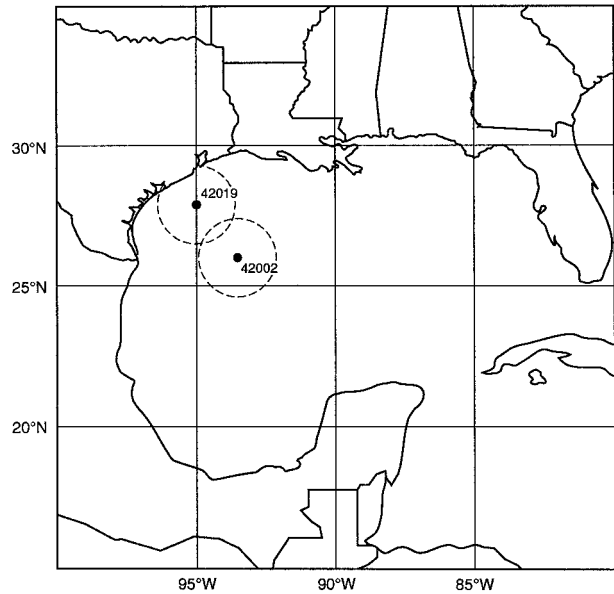

FIG. 1. The locations of NDBC buoys at stations 42019 (27.9°N, 95.0°W) and 42002 (25.9°N, 93.6°W) are shown together with collocated circles within which ship reports for search radii of 150 km were acquired. The distance separating the buoys is 263 km.

of Mexico (Fig. 1), which were equipped with the improved Rotronic MP-100 humidity sensors for the period 5 June–30 November 1993. A second Rotronic sensor was also deployed on the buoy at 42002, providing the basis for a further evaluation of these instruments. Initially, details of the sensor calibration, deployment, and reliability are addressed. Then the relative humidity and the supporting data are used to calculate specific humidities at the buoy sites. Validation for these moisture observations rely, in part, on reports from nearby ships and fixed platforms. A number of synoptic events occurred during the measurement period, which provided an opportunity to examine the response of the instrument to these events. Additionally, surface fluxes of heat and moisture using bulk parameterizations plus selected wave parameters were calculated from the buoy observations and are reported elsewhere (Breaker et al. 1998, manuscript submitted to *J. Mar. Syst.*).

2. Instrument description

a. Background

The Rotronic MP-100 humidity sensor has been under development since about 1980. Although the initial design was fragile and susceptible to contamination (Crane and Boole 1988), later versions of the instrument have proven to be more rugged and less sensitive to contamination. The Rotronic MP-100 is classified as a thin-film capacitive polymer sensor (Crescenti et al. 1990). The operation of the instrument's transducer is based on the principle of capacitance change as the polymer absorbs and desorbs water vapor. A Gore-Tex filter cov-

---

[1] This value was chosen based on NDBC's experience with the HO-83 hygrometer. Since the Rotronic sensor can read up to 103% in fog and recover comparably with the HO-83 following periods of fog, an error limit somewhat higher than 103% was chosen. See the appendix for a comparison between the Rotronic and the HO-83 humidity sensors.

ers the transducer and allows water vapor (but not liquid water) to pass through it. Contaminants reduce the passage of water vapor through the filter, which can lead to erroneous reports of saturation following high-moisture events. As a result, the filter must be kept clean (van der Meulen 1988). Laboratory tests at NDBC have indicated that the time constant for this instrument is about 20 s, even at low wind speeds. The time constant appropriate for calculating specific humidity, however, depends on the time constant for the temperature sensor and is approximately 2 min. Although the Rotronic MP-100 sensor has been used with relative success to measure moisture in the marine boundary layer, certain results have indicated that earlier versions of this instrument may have suffered from hysteresis after periods of high relative humidity (Katsaros et al. 1994).

b. Deployment

Rotronic humidity sensors were installed on two NDBC buoys in the Gulf of Mexico located at 27.9°N, 95.0°W (station number 42019) and at 25.9°N, 93.6°W (station number 42002) (Fig. 1). A second Rotronic instrument was installed on the buoy at 42002 as a backup "test" package. Figure 2 shows a photograph of the instrument and the solar radiation shield to which it is connected. The solar radiation shield is a commercial unit model 41004 manufactured by the R. M. Young Company. The Rotronic sensors on each buoy are passively aspirated since power limitations preclude active aspiration. The sensor on 42019 was installed on 4 May 1993; the sensors on 42002 were installed on 4 June 1993. The Rotronic sensor at 42019 was located at a height of 3.9 m above the water line on a 6-m NOMAD buoy that points in the direction of the prevailing wind and waves. The Rotronic sensors at 42002 were located on a circular railing 3.5 m apart at a height of 9 m above the water line on a 10-m discus buoy. This buoy has no pointing preference and so is essentially omnidirectional. Diagrams of the buoys and the arrangement and spacing of instruments on each are shown in Figs. 3 (42019) and 4 (42002). The bottom depth at station 42019 is approximately 120 m, and at station 42002 it is approximately 3200 m.

c. Calibration

Figure 5 shows pre- and postcalibration data for the Rotronic instrument installed on 42019 and the "test" instrument installed on 42002.[2] These calibrations were

---

[2] One of the Rotronic sensors on 42002 provided operational data throughout its life history. We refer to this sensor as the "operational" instrument on 42002, whereas the second instrument on 42002 reported through a separate test payload and has primarily been used as a basis for comparison with the operational unit. We refer to this instrument as the "test" unit.
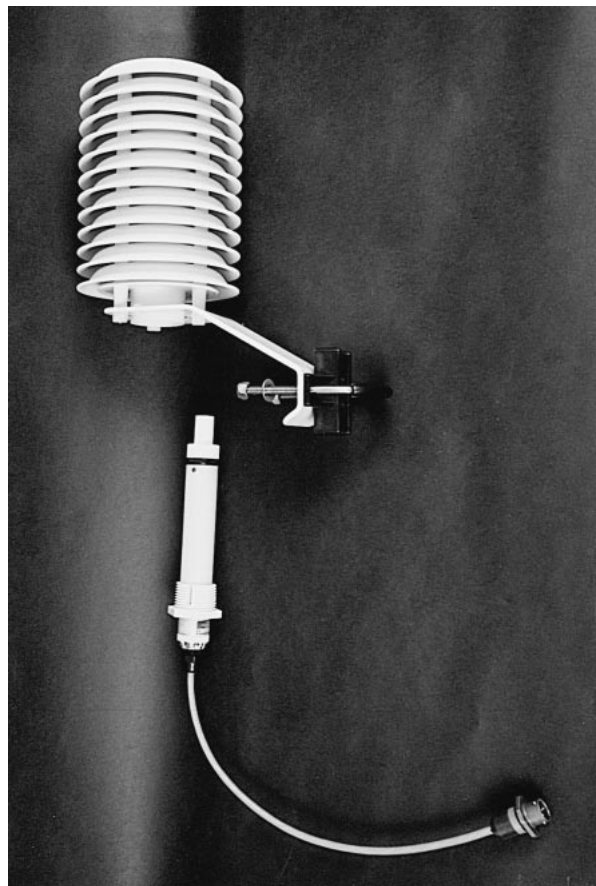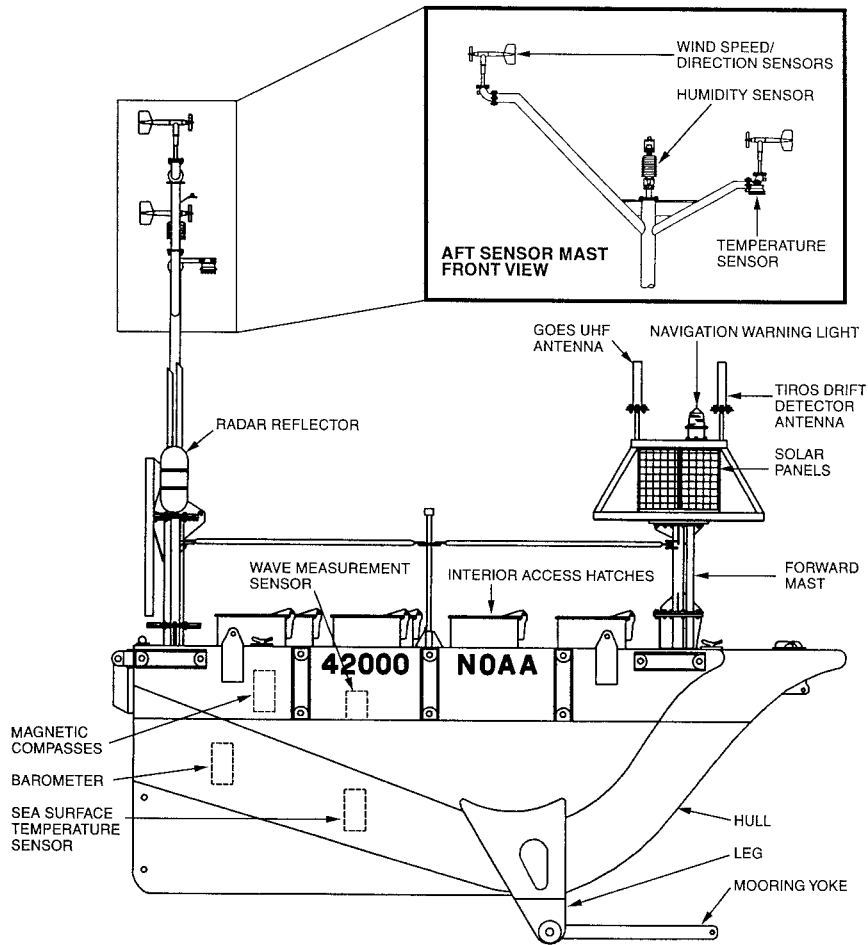

FIG. 2. Photograph of Rotronic Model 41004 sensor probe and the associated Young Multi-Plate Radiation Shield.

performed at a fixed temperature. Since the Rotronic sensor compensates for changes in temperature, its output is adjusted accordingly. Consistent with recommendations from the manufacturer, we have applied a linear fit to the calibration data. Also, the solar shielding was removed before the postcalibrations were performed because the shields did not fit inside the chamber. However, the calibrations were done with the filter in place since that is where accretion from salt spray occurs. These sensors were calibrated just prior to their deployment on each buoy. The sensor on 42019 functioned normally until it was retrieved in January 1994. When the sensor at 42019 was recalibrated (March 1994), there was a calibration shift of less than 2%. Most of this shift occurred at relative humidities of 70% or less. Both the pre- and postcalibrations for 42019 agreed with the reference values and fell within the WMO accuracy standards (shown by the dashed lines in Fig. 5), which require accuracies of ±5% for relative humidities up to 50%, and ±2% for relative humidities above 50% (WMO 1983). The test Rotronic sensor at station 42002 also operated continuously during the overall measurement period and was removed and recalibrated in August 1994. The pre- and postcalibrations for that in-

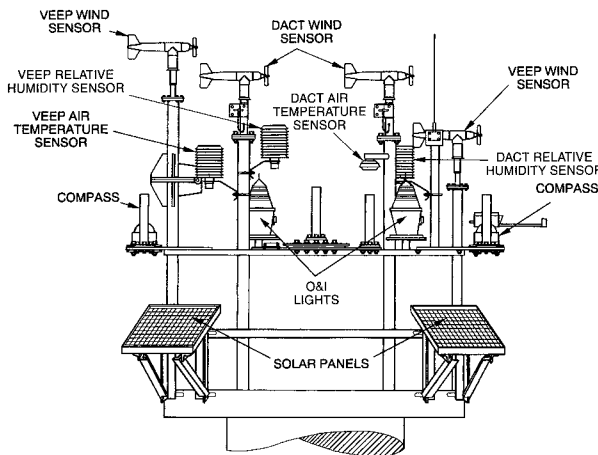FIG. 3. Sensor locations on the NOMAD buoy located at 42019.

FIG. 4. Sensor locations at the 10-m platform level on the 10-m discus buoy located at 42002. DACT and VEEP refer to the two sensor payloads that were on board. Most of the data presented in the text with the exception of the second hygrometer (referred to as "test" in the text) was from the DACT sensor payload.

strument also satisfied the WMO standards for accuracy, although there was a slight degradation in accuracy for the postcalibration at relative humidities above 80%.

d. Reliability

Since the Rotronic sensors were first installed on NDBC buoys along the West Coast, their reliability has steadily improved. Figure 6 shows the percentage of instruments that survived more than 6 months as a function of the year the sensor was deployed. This percentage increased from 18% in 1990 to 60% between 1992 and 1994 because of improved cabling and calibration. The mean time between failures for sensors deployed since 1991 is 8 months. Thus, it has not been possible to obtain useful postcalibration data for the Rotronic instruments that have been deployed in most cases because NDBC is usually only able to service each buoy every 12–24 months. Figure 7 examines these percentages based on buoy hull type. The survival percentages on the small buoys are almost identical to those on the larger 10D buoys even though exposure of the sensor to salt spray is obviously greater on the 3D and
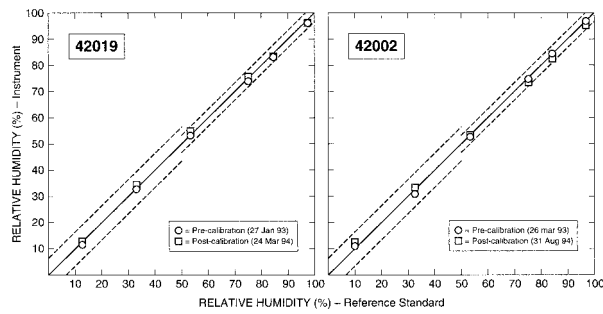
FIG. 5. Pre- and postcalibration data for the Rotronic humidity sensors installed on the buoys at stations 42019 and 42002 just prior to, and just following, the period of observation (5 June–30 November 1993). The dashed lines indicate the accuracy limits established by the WMO for humidity sensors. Pre- and postcalibrations for both sensors fall within the specified limits.
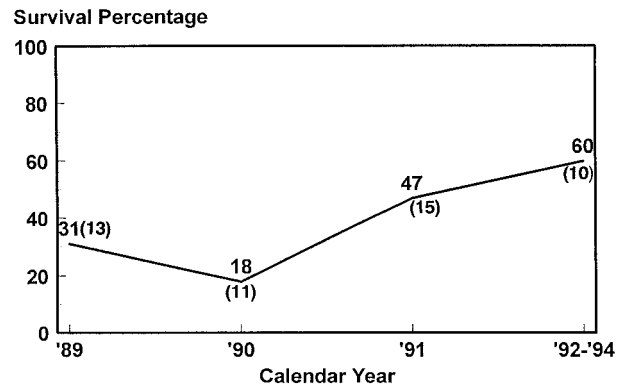

FIG. 6. Reliability of the Rotronic sensors deployed on various NDBC buoys is indicated by the percentage of instruments that survived for more than 6 months as a function of the year when the sensor was deployed. See text for additional information.

the 6N buoys. This survival pattern has not changed with time and is significant because most of the new buoys that are being deployed by NDBC are either the 3D or the 6N hull types.

3. Data acquisition and analysis

a. Acquisition

The following environmental parameters were acquired from the buoys at stations 42019 and 42002: barometric pressure, 8-min-average wind speed and direction, air temperature, sea surface temperature, and relative humidity (surface gravity wave spectra were also acquired at each buoy but are not reported here). The winds at 42019 were acquired at an elevation of 4.9 m, air temperature at 3.7 m, and humidity at 3.9 m above the surface. The winds at 42002 were acquired at an elevation of 10.0 m, air temperature at 9.6 m, and humidity at 9.0 m above the surface. Wind speed, air temperature, and specific humidity (calculated from barometric pressure, temperature, and relative humidity) at both buoys were scaled to a reference height of 10 m using standard logarithmic profile relations (e.g., Panofsky and Dutton 1984). To accomplish the scaling, a parameterization for the required roughness length z_0 employed a Charnock constant of 0.0185 (Wu 1980). Near-neutral conditions for stability within the surface boundary were assumed throughout. Barometric pressure at the buoys, which was measured at sea level (0 m), was converted to a height of 10 m using the hydrostatic equation. The observations were acquired hourly and extend from 0000 UTC 5 June to 2300 UTC 30 November 1993, spanning a period of nearly 6 months. Less than 0.5% of the data did not meet NDBC's standards for quality control[3] or were missing.

In these cases, previous values were either repeated or linear interpolation was used to fill in the missing data or to replace erroneous data in order to complete the time series. (Interpolated values were not used in making the detailed comparisons between the specific humidities derived from the two Rotronic sensors on 42002, however. In this case comparisons were made only when observed values were available from both instruments.) Sea surface temperature is measured through the hull at a depth of 1 m by a thermistor insulated from the interior hull environment.

b. The moisture calculations

Specific humidities were calculated according to Gill (1982), where the specific humidity of the air is given by

$$q_a = (0.62197e_a)/(P - 0.378e_a),$$

and the specific humidity at the ocean surface is given by

$$q_w = (0.62197e_w)/(P - 0.378e_w),$$

assuming that the air is saturated at the surface. Here, q_a and q_w are expressed in grams of water vapor per kilogram of moist air, e_a represents the vapor pressure of air (hPa), e_w is the vapor pressure (hPa) at the temperature of the ocean surface, and P is the barometric pressure (hPa) at sea level.

In turn, e_a is calculated according to

$$e_a = \text{RH}e_s/100.0,$$

where RH is the relative humidity in percent, and e_s is

---

[3] Quality control of humidity data at NDBC includes automatic flagging of the data for which the relative humidity (RH) is less than

0% or greater than 102%, and a time continuity check for which the change in RH must be less than or equal to 25% per hour. Temperature–dewpoint inversions are also flagged. Finally, all flags that are raised automatically are checked manually (T. Mettlach 1996, personal communication).
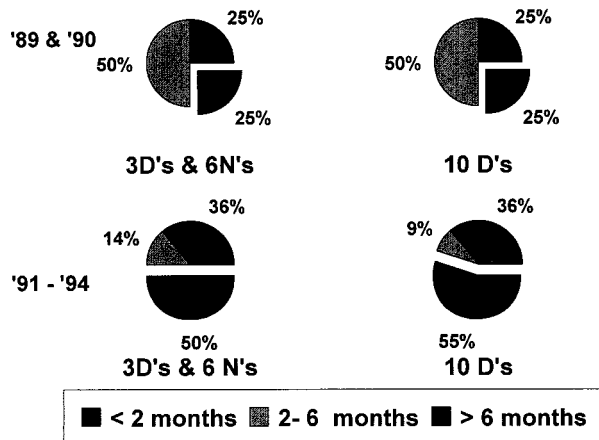
FIG. 7. Survival percentages as a function of hull type. The number of instruments used in the calculations for each time period are shown in parentheses. Note that the survival percentages for the smaller 3D and 6N buoy hull types are almost the same as for the larger 10D buoy hull type.

TABLE 1. Cross and autostatistics for the two Rotronic humidity sensors on 42002 and for 42019. All humidity values have been converted to specific humidity (gm kg^{-1}). The rmsd is the root-mean-square difference, and N is the sample size.

	Autostatistics		
Parameters	42002 (operational)	42002 (test)	42019
N	4264	4219	4296
Mean	17.13	17.57	18.42
Standard deviation	3.01	3.03	3.87
Standard deviation of the mean	4.62×10^{-2} (0.269%)	4.66×10^{-2} (0.265%)	5.90×10^{-2} (0.320%)
Minimum value	5.53	5.76	4.62
Maximum value	21.04	21.82	23.59

Cross statistics between two sensors on 42002	
N	4209
Bias (new–original)	0.438
Standard deviation	0.354
rmsd	0.563
Correlation coefficient	0.9928

the saturation vapor pressure of the air at 10 m (List 1966); e_w is computed from

$$e_w = K \times 10^v[1.0 + 1.0 \times 10^{-6}P(4.5 + 0.0006T_o^2)],$$

where T_o is the sea surface temperature (°C), v is computed from

$$v = (0.7859 + 0.03477T_o)/(1.0 + 0.00412T_o),$$

and K is a reduction factor for saturation vapor pressure over seawater. At a salinity of 35 parts per thousand (assumed here), K is taken to be 0.98 (Kraus and Businger 1994). The formulas and coefficients given above are primarily based on information contained in the Smithsonian Meteorological Tables (List 1966).

4. Results

a. Validation

NDBC has compared the Rotronic humidity sensor to an HO-83 hygrometer to determine how comparable the Rotronic's measurements were to one that is in operational use. Collocated humidity measurements were acquired for 1 month, a period during which 12 fog events occurred. Details of this comparison are presented in the appendix. The comparison was not performed to determine absolute accuracy, but to show comparability. Both instruments gave similar results overall; however, in two cases where the Rotronic instrument was saturated by fog for extended periods, it took 2–3 h longer for this sensor to recover than it did

for the HO-83 hygrometer. Because no reference data were available during the measurement period, it is not clear which instrument performed better during these periods of saturation.

To initially validate the measurements made by the Rotronic humidity sensors on the buoys, the two instruments deployed on the buoy at station 42002 have been compared. The results, given in terms of specific humidity, are summarized in Table 1. The mean difference or bias between the instruments over the entire measurement period is 4.38×10^{-1} gm kg^{-1}, or about 2.5% of the mean value, and the root-mean-square difference is 5.63×10^{-1} gm kg^{-1}. The linear coefficient of correlation between the specific humidities from the two instruments is 0.993 and is highly significant. Although close agreement was expected, this does not preclude the possibility that both instruments experienced similar systematic errors. It should be noted that the postcalibration of the test instrument on 42002 satisfied the WMO standards for accuracy, and, therefore, any systematic errors experienced would have been very small.

To estimate the error variance or uncertainty in the humidity measurements, we have used two independent approaches (Table 1). First, the uncertainties were estimated by calculating the standard deviation of the means for each record (one from 42019 and two from 42002). We could have started with the uncertainties for barometric pressure, air temperature, and relative hu-

$\rightarrow$

FIG. 8. Scatterplots comparing specific humidities from each buoy with specific humidities reported by nearby ships located within 175 km of each buoy. Numbers in the scatterplots indicate the number of times that repeated matchup values of specific humidity occurred.

Specific Humidity Matchups for Buoy 42019

Specific Humidity Matchups for Buoy 42002
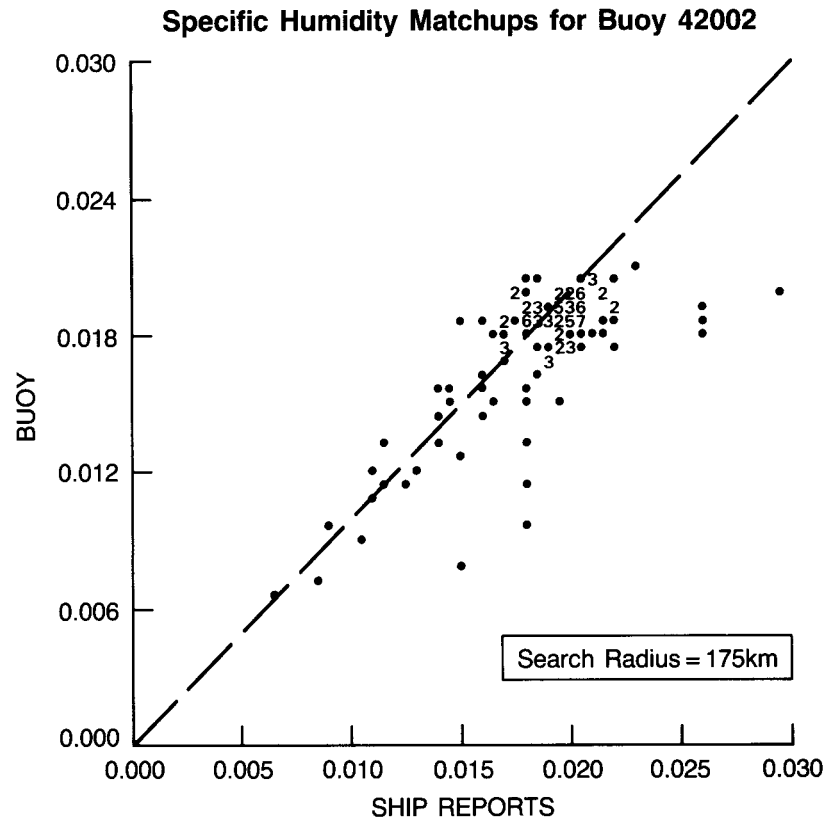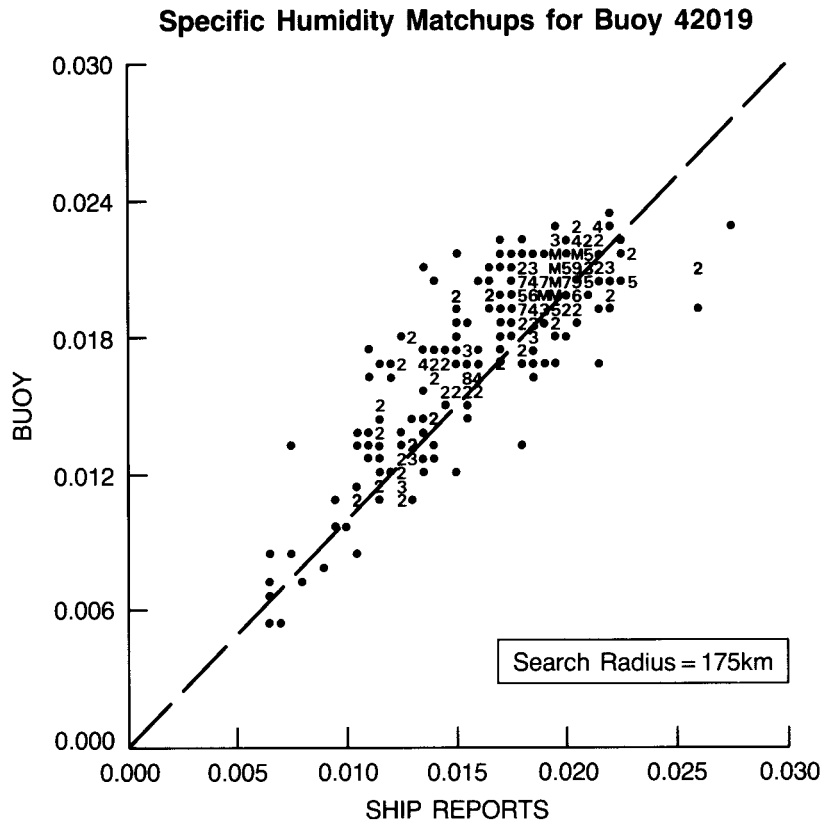
midity, and then propagated these values through the equations that were used to calculate specific humidity.[4] However, as shown by Taylor (1982), an equivalent and simpler approach in our case was simply to calculate the standard deviation of the mean values of specific humidity directly. These values range from 0.27% to 0.32% of the mean specific humidities. An entirely different approach to estimating the uncertainty in specific humidity, based on the data acquired at 42002, is to calculate the standard deviation of the differences between the two collocated instruments, which were presumably measuring the same moisture field. This calculation yielded a value of about 3.5×10^{-1} gm kg^{-1} (approximately 2.1% of the mean values involved). Our preference lies with the latter value due to the manner in which it was obtained.

To provide an independent measure of validation for the observations of moisture acquired from the buoy-mounted Rotronic humidity sensors, we have made comparisons of the buoy data (using the one sensor on 42019 and the ''operational'' sensor on 42002) with measurements of boundary layer moisture acquired from selected ships and fixed platforms (primarily oil rigs) in the surrounding area. The majority of ship reports came from two NOAA research vessels (*OREGON II* and *CHAPMAN*), which were at sea in the Gulf of Mexico during the study period. Each vessel was equipped with wet and dry bulb thermometers and used standard WMO data collection and reporting procedures.

All of the reported moisture values obtained from the ships and fixed platforms were converted to specific humidities for direct comparison with the calculated specific humidities from the buoys. Since the observing heights of the moisture measurements aboard ship were not known in a number of cases, no adjustments to a standard height were made for either the ship reports or the buoy measurements. The observations from each source were matched to within 1 h in time and were made over a range of search radii from each of the buoys (we refer to these matched pairs of ship/platform reports and buoy observations as matchups, hereafter, and no attempt was made to further stratify these data according to weather type). The search radii were increased in 25-km steps from 50 out to 300 km for each buoy. The choice of search radii was based on 1) an *e*-folding correlation distance for specific humidity of approximately 800 km in the northern Gulf of Mexico (see the following section for details) and 2) the need for adequate sample sizes. Figure 1 shows matchup circles

TABLE 2. Comparisons of specific humidities at NDBC buoys 42019 and 42002 (DACT payload) with those computed from nearby ship and fixed platform observations at various radii from each buoy.

Range (km)	Sample size	Bias (gm kg)$^{-1}$	rms (gm kg)$^{-1}$	Correlation coefficient
		Station 42019		
50	49	0.43	1.33	0.932
100	170	0.59	1.66	0.893
150	326	0.89	2.00	0.868
200	472	0.81	2.04	0.867
250	622	0.73	2.00	0.867
300	733	0.67	2.02	0.852
		Station 42002		
50	8	−1.67	2.20	0.780
100	33	−1.32	2.23	0.550
150	101	−1.46	2.76	0.712
200	166	−0.98	2.37	0.728
250	333	−0.84	2.14	0.786
300	580	−0.71	2.24	0.780

for each buoy with search radii of 150 km. Scatterplots for matchups within a search radius of 175 km of each buoy are shown in Fig. 8. Biases, rms differences, and correlations between the buoys and the ship reports are given in Table 2 for search radii of 50 to 300 km (in 50-km steps). The statistics become repeatable (i.e., stabilize) at sample sizes of the order of 300, which correspond to search radii of 150 and 250 km for buoys 42019 and 42002, respectively. In all cases where sample sizes exceeded 33, the correlation coefficients between the buoys and the ship reports exceeded 0.70 and were statistically significant at the 99% level of confidence. Although the values of moisture obtained from the buoy at 42019 on average tend to be slightly higher than the ship reports (indicated by the positive biases), the opposite is true for the operational sensor on buoy 42002. Also, the rms differences are slightly higher and the correlations lower for the sensor on buoy 42002. Because the differences between the buoy and the ship reports are only slightly greater than, but still of the same order as, the height adjustments that could have been applied, if the observing heights had been available, we can make no definitive statement concerning their significance.

In 1986, Katsaros et al. (1994) conducted field tests on a number of humidity sensors including the Rotronic MP-100 instrument. Hysteresis was found to occur for mean humidities following high-moisture events for the Rotronic MP-100 instrument. The greatest differences between the Rotronic sensor and a reference psychrometer occurred at relative humidities less than 70%, particularly after periods of high relative humidity. The Rotronic sensor apparently required time to dry out after periods of high moisture. Finally, a bias of 8% between the Rotronic MP-100 and a reference psychrometer was

---

[4] See Gilhousen (1987) for estimates of accuracy for barometric pressure, air temperature, and sea surface temperature. According to the manufacturer, the accuracy for RH is ±1.5% at 40°C for 0 ≤ RH ≤ 100, ±1.3% at 20°C for 0 ≤ RH ≤ 100, and ±2.0% at 0°C for 0 ≤ RH ≤ 100.

not due simply to a calibration error but was attributed in part to hysteresis by the sensor.[5]

To address the problem raised by Katsaros et al., we first looked for periods of high relative humidity in our data. Cumulative distributions of relative humidity for each buoy (not shown) indicate that only about 8% of the data from either buoy have relative humidities that exceed 90%, and only about 2% of the data exceed 95%. Overall, very few periods of identifiable rain occurred during the study period, and those periods that could be identified did not coincide precisely with any of our ship reports. To examine the hysteresis problem adequately with our data would have required locating matchups that occurred within a narrow window of several hours following clearly defined high moisture (i.e., saturation) events and, as indicated, no such matchups were found. Our comparisons with the ship reports above, however, showed only small biases (3.6% for 42019 and −4.1% for 42002). If hysteresis was a serious problem, we might have expected both biases to be positive (i.e., buoys to be higher than the ship reports) due to the fictitiously higher values that persisted during the periods when the instrument should have already recovered. This result, of course, was also influenced by the fact that high relative humidities (greater than approximately 95%) were an unusual occurrence in our data. In summary, our data are not adequate to address the hysteresis problem raised by Katsaros et al. (1994). However, based on the limited data available, no evidence for a significant hysteresis problem could be found for the Rotronic sensors deployed on buoys 42019 and 42002. Also, the observations presented by Katsaros et al. were acquired in 1986, and several improvements were made to the instrument by the manufacturer in the late 1980s including 1) a change to the polymer to improve its ability to resist a variety of contaminants and 2) the filter was changed from steel to Gore-Tex to prevent penetration of salt particles (F. Fetkowitz 1996, personal communication). Finally, based on the results of Visscher and Schurer (1985), Muller and Beekman (1987), and Hundermark (1989), hysteresis problems were not previously found with the Rotronic MP-100 instrument.

b. Temporal variability of environmental parameters

Sea level pressure, wind speed, wind direction, sea surface temperature, air temperature, and relative humidity were acquired directly from sensors on the buoys.

Time series plots of the first five parameters are shown in Figs. 9 (42019) and 10 (42002). All atmospheric observations were adjusted to a height of 10 m, as indicated earlier. From these figures, it is evident that temporal variability occurs on three scales: meso (on the order of hours), synoptic (several days), and seasonal (several months).

During the months of June through August 1993, little or no synoptic variability is noted, but, beginning in late September, synoptic-scale variability in the form of frontal incursions into the Gulf of Mexico becomes evident in the time series. Consistent with the results of DiMego et al. (1976) and Henry (1979), there is a minimum of frontal activity during the summer months and a maximum from November through March with a short, dramatic increase in frontal activity during September and October. More frontal activity occurs at 42019 than at 42002 during these months because some of the weaker fronts succumb to frontolysis before reaching 42002.

Figure 11 shows the time series of specific humidity at the surface and at 10 m for stations 42019 (upper panel) and 42002 (lower panel). Specific humidity at the surface follows sea surface temperature, upon which it is primarily based, but does not respond strongly to the atmospheric conditions above, at least on synoptic and shorter timescales. As a result, the pattern of variability that occurs at the surface is quite different from that that occurs at 10 m. Surface specific humidity in most cases exceeds that at 10 m. However, for brief periods in October and November, the specific humidity at 10 m does, in fact, exceed that at the surface at 42019 during certain return-flow events (discussed later in this section). In these cases, the surrounding air has been significantly modified through the transfer of heat and moisture from the underlying ocean surface.

Cross-correlation analyses were performed for the two buoy time series of specific humidity, wind speed, barometric pressure, air temperature, and sea surface temperature. The maximum cross correlations and the corresponding lags are presented in Table 3. The correlation coefficients consistently exceed 0.9, except for wind speed where local effects become more important. Of particular interest are the lag relationships between the time series for each parameter. Of these parameters, air temperature and specific humidity both attain their maximum correlations at lags of −6 and −7 h, respectively, whereas the other parameters are maximally correlated at, or near, zero lag. Lags of −6 or −7 h indicate that coherent sources of variation occur at 42019 prior to their occurrence at 42002, which is consistent with atmospheric disturbances that propagate from the northwest with speeds on the order of 10–15 m s^{-1}. Based on a maximum cross correlation of 0.91, a separation distance of 263 km between the buoys, and an exponential decay law, the e-folding distance for specific humidity is approximately 800 km, indicating that variations in moisture are spatially coherent over relatively large distances in the northern Gulf of Mexico.

[5] The problem raised by Katsaros et al. is not unrelated to the results presented in the appendix, where it was shown that in a few cases when the instrument was saturated for extended periods, recovery from saturation was slower than that demonstrated by an independent hygrometer. However, as indicated in the appendix, it is not clear whether the Rotronic sensor or the HO-83 was at fault in this situation.
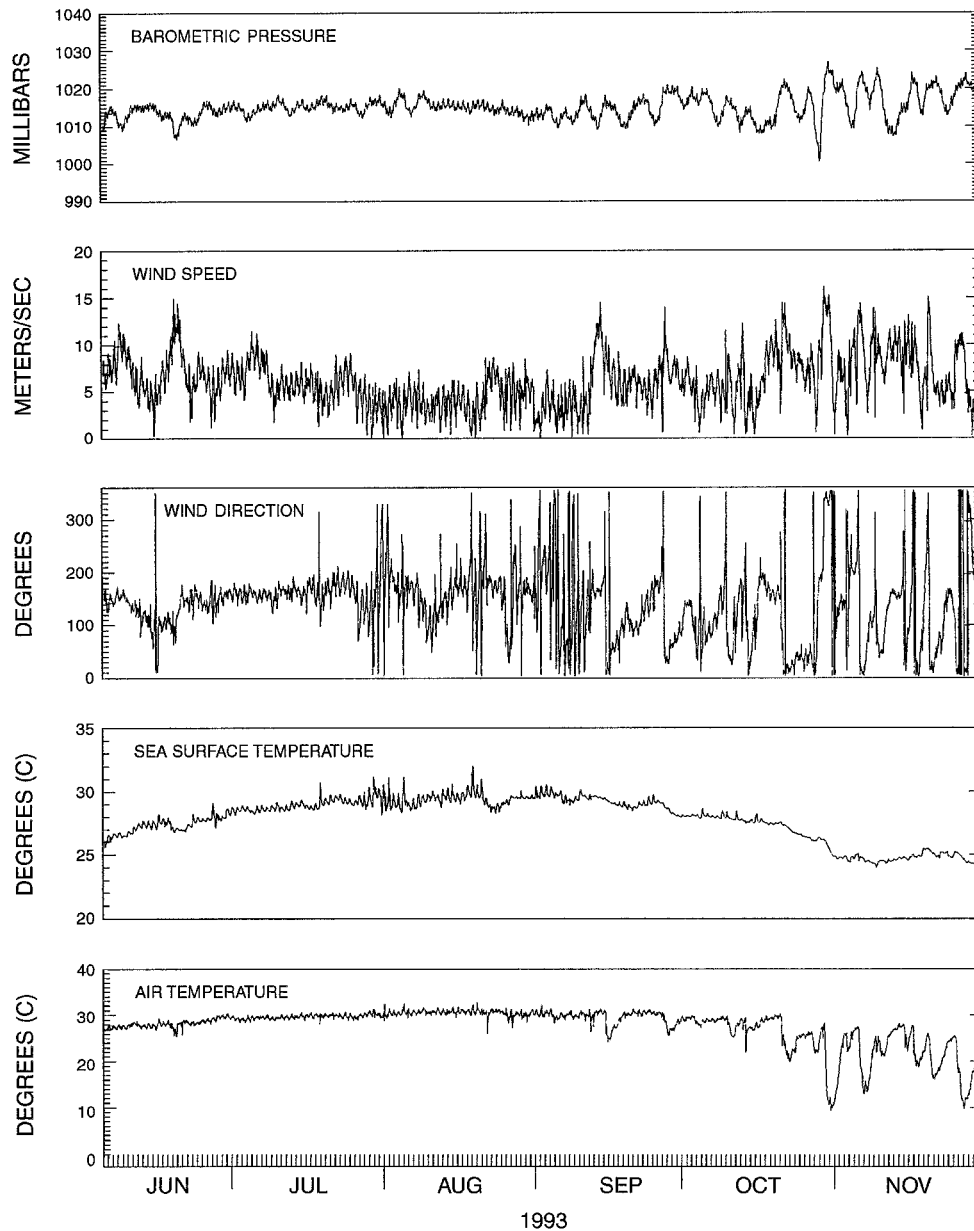
42019

FIG. 9. Time series of hourly sea level pressure, wind speed, wind direction, sea surface temperature, and air temperature are shown for the period 5 June–30 November 1993 for the buoy at station 42019.

Successive cross correlations for specific humidity were also calculated for 7-day (168 h) periods, stepping through the data hour by hour. The results are displayed in Fig. 12, where both the maximum cross correlations (upper panel) and the corresponding lags (lower panel) are shown. The maximum correlations increase abruptly around 7 September, and the lags change from mostly positive to essentially negative at this time, indicating that events prior to the first week in September generally arrived at 42002 before they arrived at 42019 and conversely thereafter. These changes in correlation structure

for specific humidity are significant and reflect a seasonal change in synoptic weather conditions in the northern Gulf of Mexico. In particular, they imply that the prevailing patterns became coherent and tended to enter the buoy domain from the north rather than from the south after the first week in September, which is in general agreement with DiMego et al. (1976) and Henry (1979).

Crisp and Lewis (1992) define the so-called return-flow cycle as the sequence of events that lead to the initiation and termination of return flow over the Gulf
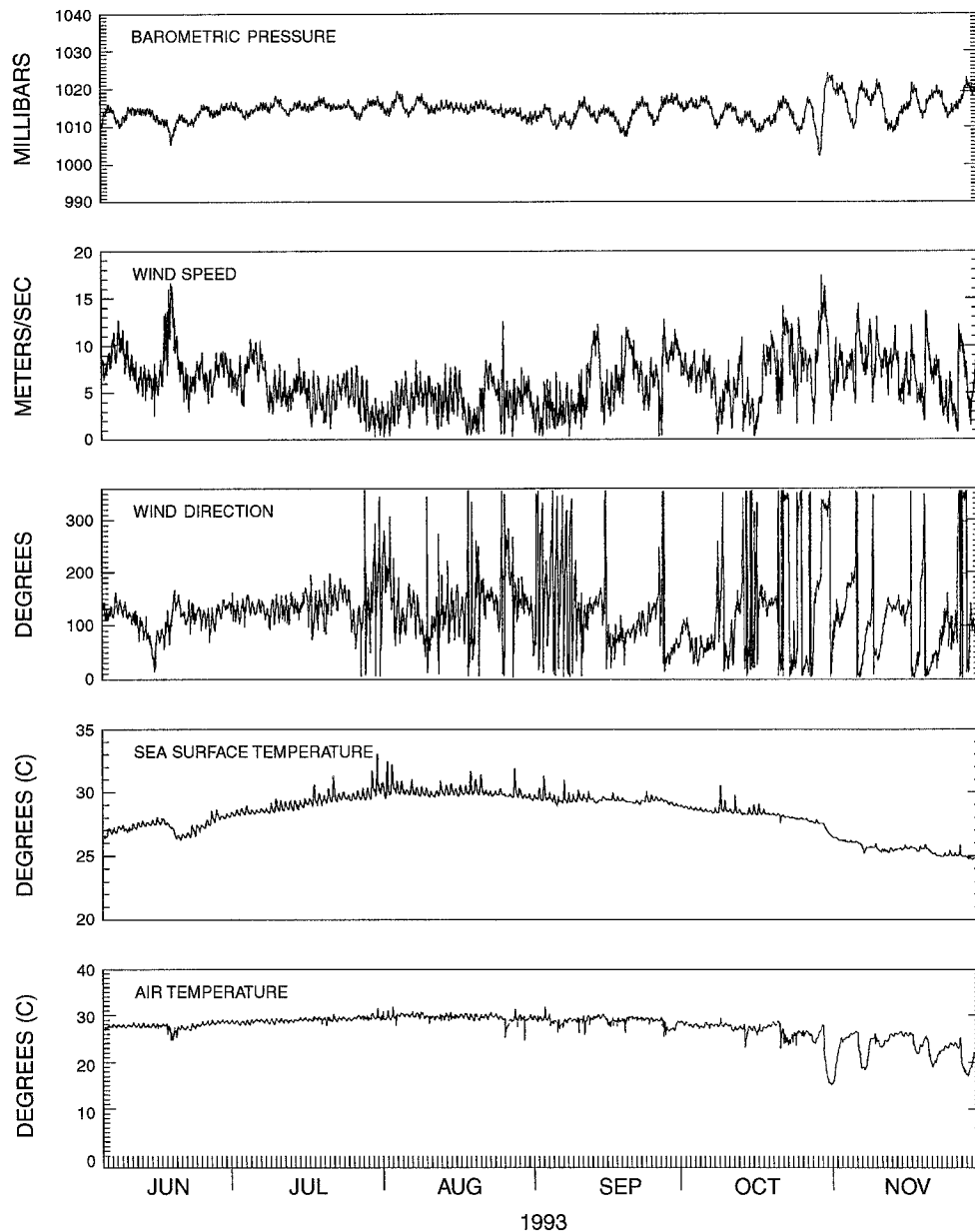
42002

FIG. 10. Same as Fig. 9 except for 42002 (DACT payload).

of Mexico. The first phase of the cycle is defined as the movement of cold, dry air from the continent to the Gulf of Mexico and is called the offshore-flow phase. The second phase is defined as the return of modified air to the continent (return-flow phase). Figure 13 illustrates in greater detail how sea level pressure, wind speed, wind direction, air temperature, and specific humidity vary at the buoys during a particular return flow event (the solid curve corresponds to buoy 42019, the dashed line to 42002). This event started early on 30 October and ended on 5 November at 42019 and on 6 November at 42002.

It is evident that a lag of 6–12 h exists between 42002 and 42019 for the parameters shown. Lags in pressure and wind speed are not apparent in the cross correlation and lag statistics given earlier (Table 3) probably because the small-scale variability in these parameters tends to mask the lag structure that emerges in the synoptic variability during individual events. Also evident is the warming and moistening that takes place between these buoys during the offshore-flow phase (approximately 4°C and approximately 2 gm kg^{-1}, respectively). The offshore-flow phase of the return-flow cycle begins at both stations on 30 October. This is associated with
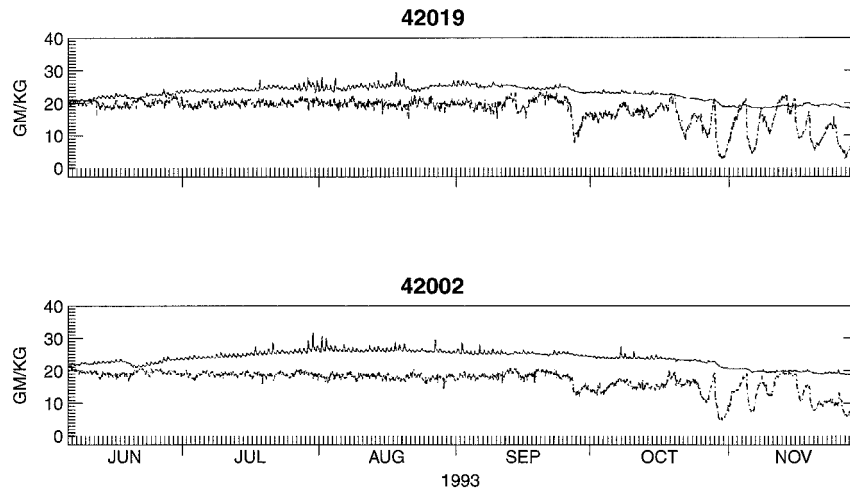
FIG. 11. The time series of specific humidity at the surface and at 10 m for the period 5 June–30 November 1993 are plotted in the upper panel for 42019 and for 42002 (DACT payload) in the lower panel. In each case, the upper trace represents specific humidity at the surface.

a pressure minimum, increased wind speed, a change from southerly to northerly winds, an abrupt drop in temperature, and an equally abrupt decrease in specific humidity. The air temperature and specific humidity reach minima on 31 October, while the pressure increases to a maximum, the wind direction becomes erratic, and the wind speed reaches a minimum.

From 1 through 2 November, the wind direction changes to southeasterly, and the wind speed increases as the high pressure ridge moves toward the southeast and farther into the Gulf of Mexico. The air temperatures and specific humidities rise, indicating that the return-flow phase of the return-flow cycle has begun. These trends continue, and the wind direction becomes more southerly at 42002 until the next return-flow cycle begins on 6 November.

On 3 November a weak cold front moves off the coast and frontolizes in the vicinity of 42019. This has the effect of producing minimal offshore flow at the buoy, which decreases the temperature, causes the wind direction to become northwesterly, and decreases the wind speed. The increase in specific humidity is reduced but not reversed. In effect, the frontolysis modulates and slows the return-flow phase of the return-flow cycle at 42019 but has little or no effect at 42002.

TABLE 3. Cross-correlation statistics for the entire series of hourly values for the environmental parameters included below from 0000 UTC 5 June to 2300 UTC 30 November 1993. *Negative sign indicates that the series at 42019 leads the series at 42002.

Environmental parameter	Cross correlation	Lag (h)*
Specific humidity	0.911	−7
Wind speed	0.678	−1
Barometric pressure	0.939	0
Air temperature	0.943	−6
Sea surface temperature	0.910	0

According to Henry (1979), fronts can enter the Gulf of Mexico in any month; however, no fronts entered the gulf during June, July, or August of 1993. In mid-June, the buoys were influenced by Tropical Storm Arlene, however, as she tracked from the Gulf of Campeche toward the U.S. mainland. In any given year, the number of fronts is highly variable, and any statistic will be somewhat sample dependent unless the sample is quite large. Henry studied the fate of fronts in the Gulf of Mexico for an 11-yr period from 1967 to 1977. He found that during the months of September, October, and November an average of 2.4, 3.7, and 5.2 fronts entered the Gulf of Mexico, respectively. For those months during 1993, 2, 3, and 4 fronts entered the Gulf.

5. Summary and conclusions

The overall reliability of the Rotronic MP-100 humidity sensors, which have been deployed on various NDBC buoys over the past 7 years, has improved significantly since 1989 when they were first considered for possible long-term deployment on fixed platforms at sea.

Over the approximate 6-month period that the Rotronic sensor installed on the buoy at station 42019 was deployed, its calibration remained within the accuracy limits set by the WMO. The ''operational'' Rotronic sensor installed at station 42002 operated continuously from its deployment in June 1993 until it finally failed in January 1997.

Katsaros et al. (1994) have reported that an earlier version of the Rotronic sensor experienced hysteresis following periods of high moisture. Our observations did not permit us to examine this question in detail. However, problems associated with hysteresis for the Rotronic sensor have not been reported elsewhere, which may be due to the fact that improvements were
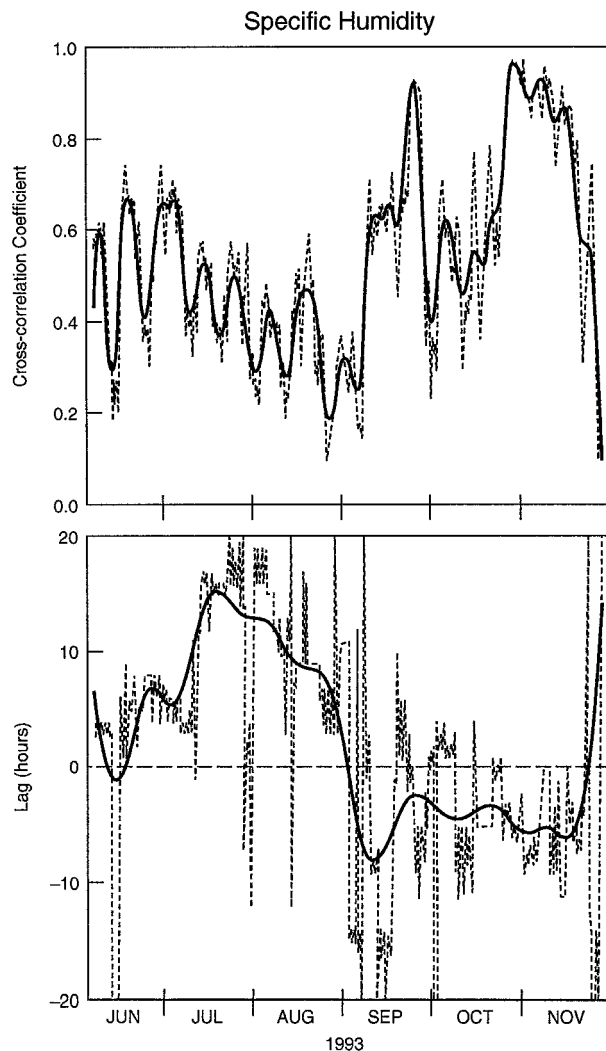
Specific Humidity

FIG. 12. Cross correlations for specific humidity between the buoys at stations 42019 and 42002 (DACT payload) at 10 m for successive 7-day segments of the time series at 1-h time increments. The maximum cross correlations are plotted in the upper panel and the corresponding lags (h) in the lower panel. The dashed curves represent the original values and the solid curves denote the results after smoothing.

made to the instrument by the manufacturer subsequent to the observations of Katsaros et al.

The buoy observations of relative humidity and supporting data from the buoys were used to calculate specific humidity. Specific humidities calculated from the buoy data were compared with specific humidities computed from observations obtained from nearby ship reports and the correlations were generally high (0.7–0.9). Uncertainties in the calculated values of specific humidity from buoys were also estimated and ranged from 0.27% to 2.1% of the mean value depending on the method used to perform the calculation.

Observations at each of the buoys acquired during this study were used to construct time series of specific humidity. The time series of specific humidity at a height

of 10 m reveal three primary scales of variability: meso (of the order of hours), synoptic (several days), and seasonal (several months). The synoptic variability was primarily due to the arrival of frontal systems with cold, dry air behind them that dropped down into the Gulf of Mexico from the continental United States and occurred primarily during September, October, and November. A particularly intense event on 30 October 1993 was selected for further analysis and displayed a characteristic return-flow cycle that often occurs during fall and winter in the northern Gulf of Mexico. In all cases, the moisture data acquired at the buoys were highly sensitive to all observable variability that took place in the marine boundary layer during the period of this study.

A cross-correlation analysis between the buoys (for a separation distance of 263 km) for specific humidity and the other buoy parameters (at 10 m) indicated that 1) all parameters were highly correlated (greater than 0.9) except for wind speed and 2) the e-folding correlation distance for specific humidity was at least 800 km. A more detailed cross-correlation analysis of the specific humidity time series revealed a major change in correlation structure that occurred during the first week in September, indicating that weather patterns became more coherent and tended to enter the northern Gulf of Mexico from the north rather than from the south, as they tended to prior to this time.

In summary, the events described above produced strong and well-defined signatures in the moisture-related observations, emphasizing the importance of these data in characterizing synoptic-scale variability in the near-surface marine environment. These observations also have definite operational utility in forecasting the return-flow events that occur in the Gulf of Mexico. As noted by Weiss (1992), much of the difficulty in forecasting severe weather in these return-flow events is that there is no information about where the high-moisture content air is located until it reaches the coastal plain. The availability of at least one humidity sensor strategically located on the continental shelf would help alleviate this problem.
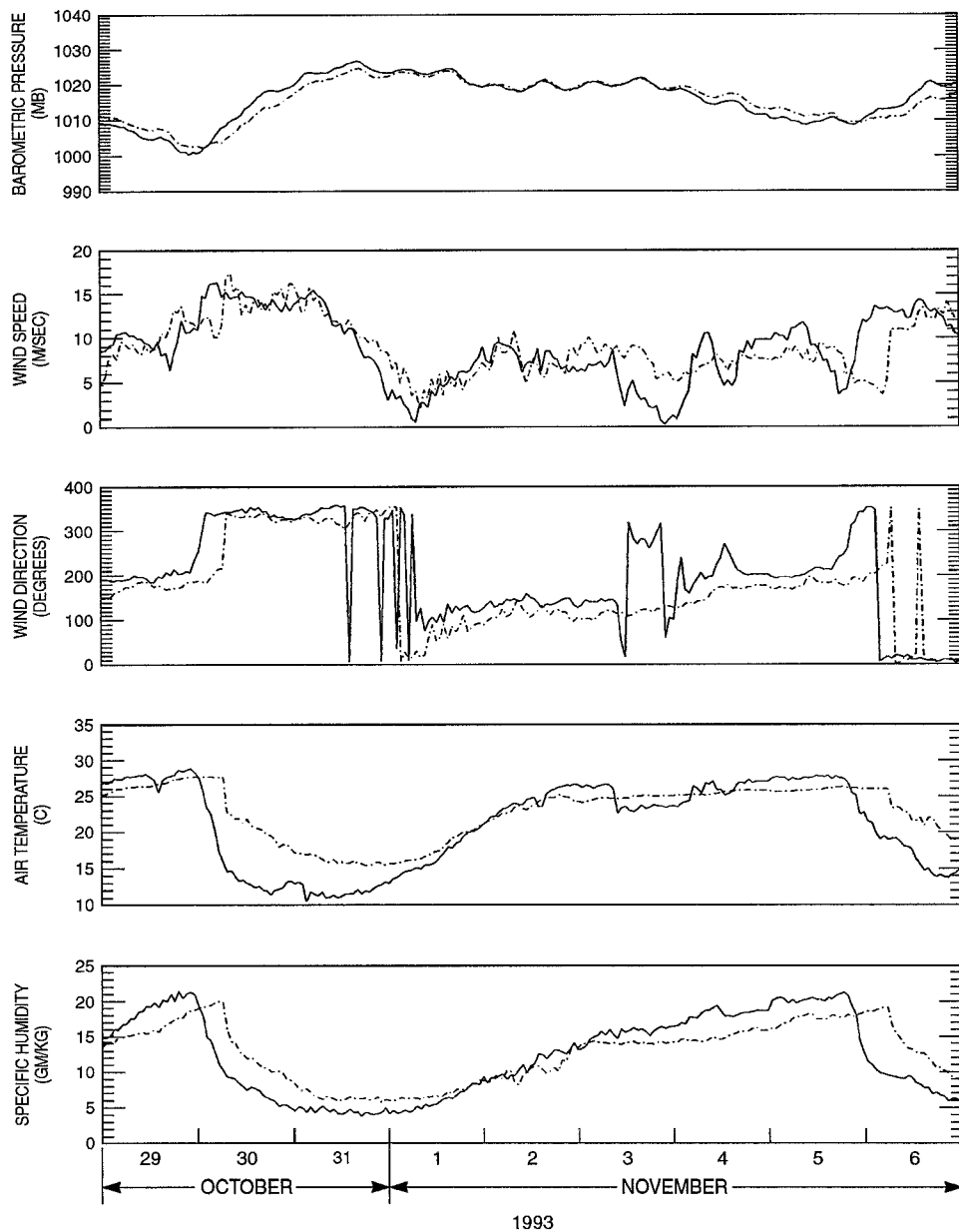
FIG. 13. Expanded time series for the return flow event of 30 October–6 November for barometric pressure, wind speed, wind direction, air temperature, and specific humidity. The solid curves refer to the observations from 42019 and the dashed curves to 42002.

APPENDIX

A Comparison between the Rotronic and HO-83 Humidity Measurements

During January 1993, relative humidities from a Rotronic MP-100 humidity sensor were compared with humidities measured by an independent HO-83 hygrometer. This instrument is a chilled-mirror system that is electronically aspirated. The HO-83 hygrometer has been used operationally by the National Weather Service since the mid-1980s and in Automated Surface Obser-

vation System units since the early 1990s. The comparison was performed to examine the comparability of the measurements from the Rotronic instrument to measurements from a hygrometer in operational use. It was not performed to determine absolute accuracy.

The comparison was conducted on a test stand in open conditions near NDBC. A number of fog or saturation events occurred, which are numbered across the top of the time series plot in Fig. A1; the measurements from the two sensors are shown for the first 12 days of the month. Both sensors were located 2 m above the ground
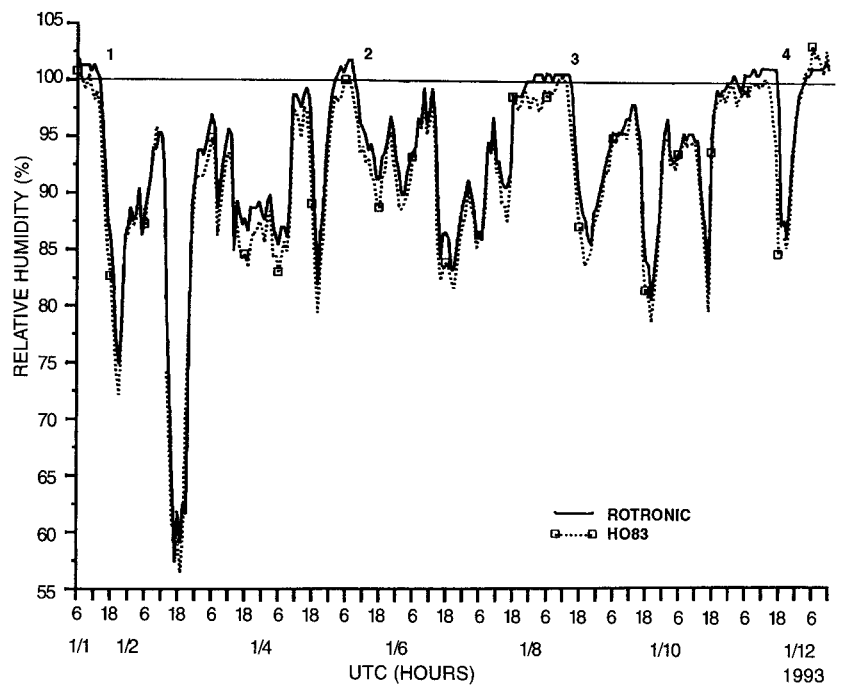
FIG. A1. Comparison of relative humidity from the HO-83 hygrometer and from the Rotronic humidity sensor for the first 12 days in January 1993. The comparison was conducted on a test stand outside on the grounds of NDBC. The sensors were within 4 m of each other at 2 m above the ground during the comparison.

and within 4 m of each other. In general, the measurements tracked well together, including periods of rapid humidity change. Overall, the Rotronic sensor reported about 1.0%–2.5% higher than the HO-83.

One apparent weakness of the Rotronic instrument, however, may occur after extended periods of saturation (fog events 3 and 4). Perhaps because of the lack of aspiration, the Rotronic unit continues to report over 100% for 2–3 h after the HO-83 reports an abrupt drop in humidity. The Rotronic measurements do not show any shift in bias compared to the HO-83 after the fog events, however. This conclusion is also supported by the comparison statistics presented in Table A1, which include data for the entire month. Although there were 12 fog events during the month, only 2 of the 12 events (events 3 and 4) showed any significant differences. The problem of continuing to report humidities over 100% may be confined to cases when fog events persist for

over 12 h and the winds remain calm. It should be noted that the HO-83, because it is a chilled mirror device, has difficulty maintaining a contaminant-free mirror and, therefore, needs frequent cleaning. Consequently, it is also possible that the HO-83 hygrometer may have been reporting incorrectly during these periods of extended fog rather than the Rotronic instrument.

REFERENCES

Breaker, L. C., D. B. Gilhousen, H. L. Tolman, and L. D. Burroughs, 1998: Initial results from long-term measurements of atmospheric humidity and related parameters in the marine boundary layer at two locations in the Gulf of Mexico. *J. Mar. Syst.,* in press.

Coantic, M., and C. A. Friehe, 1980: Slow-response humidity sensors. *Air–Sea Interaction in Instruments and Methods,* F. Dobson, L. Hasse, and R. Davis, Eds., Plenum Press, 399–411.

Crane, J., and D. Boole, 1988: Thin film humidity sensors: A rising technology. *Sensors,* **5,** 32–35.

Crescenti, G. H., R. E. Payne, and R. A. Weller, 1990: Improved meteorological measurements from buoys and ships (IMET): Preliminary comparison of humidity sensors. Woods Hole Tech. Rep. WHOI-90–18, 57 pp. [Available from Document Library, Woods Hole Oceanographic Institution, Woods Hole, MA 02543.]

Crisp, C. A., and J. M. Lewis, 1992: Return flow in the Gulf of Mexico. Part I: A classificatory approach with a global historical perspective. *J. Appl. Meteor.,* **31,** 868–881.

DiMego, G. J., L. F. Bosart, and G. W. Endersen, 1976: An examination of the frequency and mean conditions surrounding frontal incursions into the Gulf of Mexico and Caribbean Sea. *Mon. Wea. Rev.,* **104,** 709–718.

TABLE A1. Summary statistics showing the relative humidity differences between a Rotronic and an HO-83. Bias is given by Rotronic–HO-83. Here, σ is the standard deviation and N is the number of cases.

	Relative humidity difference (%)		
	Bias	σ	N
Overall	1.2	0.5	744
Before event 3	1.4	0.7	162
After event 4	1.3	0.6	456

Gilhousen, D. B., 1987: A field evaluation of NDBC moored buoy winds. *J. Atmos. Oceanic Technol.,* **4,** 94–104.

Gill, A. E., 1982: *Atmosphere–Ocean Dynamics.* Vol. 30, *International Geophysics Series,* Academic Press, 662 pp.

Henry, W. K., 1979: Some aspects of the fate of cold fronts in the Gulf of Mexico. *Mon. Wea. Rev.,* **107,** 1078–1082.

Hundermark, B. W., 1989: Field evaluation of the Rotronic humidity sensor and the impulsphysik visibility sensor. *Proc. Conf. and Exposition on Marine Data Systems,* New Orleans, LA, Mar. Tech. Soc., 81–85.

Katsaros, K. B., and Coauthors, 1994: Measurements of humidity and temperature in the marine environment during the HEXOS main experiment. *J. Atmos. Oceanic Technol.,* **11,** 964–981.

Kraus, E. B., and J. A. Businger, 1994: *Atmosphere–Ocean Interaction.* 2d ed. Clarendon Press, 362 pp.

List, R. J., 1966: *Smithsonian Meteorological Tables.* Smithsonian Institution, 527 pp.

Muller, S. A., and P. J. Beekman, 1987: A test of commercial humidity sensors for use at automatic weather stations. *J. Atmos. Oceanic Technol.,* **4,** 731–735.

Panofsky, H. A., and J. A. Dutton, 1984: *Atmospheric Turbulence.* Wiley, 397 pp.

Semmer, S. R., 1987: Evaluation of a capacitance humidity sensor. *Sixth Symp. on Meteor. Observations and Instrumentation,* New Orleans, LA, Amer. Meteor. Soc., 223–225.

Taylor, J. R., 1982: *An Introduction to Error Analysis.* University Science Books, 270 pp.

van der Meulen, J. P., 1988: On the need of appropriate filter techniques to be considered using electrical humidity sensors. *Proc. WMO Tech. Conf. on Instruments and Methods of Observation (TECO-1988),* Leipzig, Germany, World Meteor. Org., 55–60.

Visscher, G. J. W., and K. Schurer, 1985: Some research on the stability of several capacitive thin film (polymer) humidity sensors in practice. *Proc. 1985 Int. Symp. on Moisture and Humidity,* Washington, DC, Instrument Soc. Amer., 515–523.

Weiss, S. J., 1992: Some aspects of forecasting severe thunderstorms during cool-season return-flow episodes. *J. Appl. Meteor.,* **31,** 964–982.

World Meteorological Organization, 1983: Measurement of atmospheric humidity. *Guide to Meteorological Instruments and Methods of Observation,* 5th ed., World Meteor. Org., 5.1–5.12.

Wu, J., 1980: Wind-stress coefficients over sea surface near neutral conditions—A revisit. *J. Phys. Oceanogr.,* **10,** 727–740.